

## Effect of plasma waves on the optical properties of a multilayered metallic Fibonacci superlattice

Wei-guo Feng

*International Centre for Theoretical Physics, Trieste, Italy  
and Pohl Institute of Solid State Physics, Tongji University, Shanghai 200 092, People's Republic of China*

Nian-hua Liu

*Department of Physics, Ji-An Teachers Training College, Ji-An, Jiangxi 343 009, People's Republic of China*

Xiang Wu

*Centre of Theoretical Physics, Chinese Center of Advanced Science and Technology (World Laboratory),  
P. O. Box 8730, Beijing, People's Republic of China;*

*International Centre for Materials Physics, Academia Sinica, Shenyang, People's Republic of China;  
and Pohl Institute of Solid State Physics, Tongji University, Shanghai 200 092, People's Republic of China*

(Received 16 July 1990)

Within the hydrodynamic model of electron dynamics, the optical properties of a metallic Fibonacci superlattice have been studied for the region of  $p$ -polarized soft x rays and the extreme ultraviolet. By using the  $4 \times 4$  transfer-matrix formalism and taking into account retardation effects and the coupling between transverse and longitudinal waves at the metal boundaries, we have discussed the electromagnetic normal modes for the quasiperiodic superlattice in the rational approximation. We found that the dispersion curves are mainly of two types, and, similar to the reflectivities, both the real and imaginary parts of the dispersion-relation pattern have a rich structure of self-similarity. With increasing generation number, the electromagnetic modes all become critical.

### I. INTRODUCTION

In the past few years, many scientists have become very interested in the optical properties of periodic and quasiperiodic superlattices.<sup>1-12</sup> Based on the hydrodynamic model and the transfer-matrix method, by taking into account plasma-wave spatial dispersion and retardation, and using the additional boundary condition (ABC),<sup>13</sup> Mochàn and Castillo-Mussot<sup>6</sup> studied the dispersion relation of the electromagnetic normal modes and the reflectivities of infinite conductor-insulator and conductor-conductor periodic superlattices, and obtained a variety of modes made up of interacting surface and bulk plasmons, which yield a rich structure in the reflectance spectra. Kohmoto, Sutherland, and Iguchi<sup>8</sup> proposed an experiment to probe the (quasi) localization of the phonon, in which the optical layers are constructed following the Fibonacci sequence.<sup>9</sup> The consequent numerical results reveal that the transmission coefficient has also a rich structure and is multifractal. Recently, we calculated the reflection of  $s$ -polarized soft x rays and the extreme ultraviolet from a metallic Fibonacci superlattice (MFSL).<sup>14,15</sup> We found that the calculated reflection spectra are of the interesting self-similarity pattern, some strong reflection peaks move to a higher-frequency region compared with the usual periodic superlattice, which stimulates the interest in the study and making of soft x rays and extreme ultraviolet reflectors. Later we made a further study of the dispersion behavior of the electromagnetic normal modes for the  $s$ -polarized waves in

the rational approximation.<sup>16,17</sup> We revealed that both the real and imaginary parts of the dispersion curves are of self-similarity, the scaling of which is the same as that in the situation of the reflection spectra. In this paper we will discuss the case of  $p$ -polarized electromagnetic waves by taking into account the coupling between transverse and longitudinal waves at the metal boundaries, and present a general formalism for the calculation of the dispersion relation of the electromagnetic normal modes in the rational approximation for the  $n$ th generation MFSL.

### II. GENERAL FORMALISM OF THE DISPERSION RELATION FOR THE $p$ -POLARIZED ELECTROMAGNETIC WAVE

The Fibonacci superlattice structure, which was first presented by Merlin *et al.*,<sup>9</sup> can be constructed by stacking recursively along the  $z$  direction with two generators, blocks  $L$  and  $S$ , mapping the mathematical rule in the Fibonacci sequence, i.e.,

$$S_1 = \{L\}, \quad S_2 = \{LS\}, \quad S_3 = \{LSL\}, \dots, \quad (1)$$

$$S_n = S_{n-1}S_{n-2}.$$

In the case of MFSL, each block contains the same two kinds of metallic layers  $A$  and  $B$ . The thickness of the layer  $A$ , which is denoted as  $d_A$ , in block  $L$  is the same as in block  $S$ , but the thicknesses for layer  $B$  in the two blocks are of different values, which are denoted as  $d_{BL}$

and  $d_{BS}$  for the two blocks, respectively. As adopted in Ref. 14, the ratio of the thickness of the two elementary blocks is just the inverse of the golden mean,

$$\Lambda \equiv \frac{d_A + d_{BS}}{d_A + d_{BL}} = \frac{\sqrt{5}-1}{2}. \quad (2)$$

For an  $n$ th generation MFSL, we have  $N=2F_n$  metal layers, where  $F_n$  is the  $n$ th order of the Fibonacci sequence, which is defined as

$$F_0=1, F_1=1, F_2=2, \dots, F_n=F_{n-1}+F_{n-2}. \quad (3)$$

The total thickness of the  $n$ th MFSL can be expressed as

$$D_n=(F_{n-1}+\Lambda F_{n-2})(d_A+d_{BL}). \quad (4)$$

As the  $s$ -polarized electromagnetic waves do not couple to plasmons,<sup>6</sup> we will only discuss the situation of the  $p$ -polarized waves. Let us now consider a general case of a metal layer of thickness  $d_\mu$  in the MFSL, in which there exist two kinds of  $p$ -polarized electromagnetic waves, the reflectance (left moving) and transmission (right moving) waves, the wave vectors of which lie on the  $x$ - $z$  plane and take the values as

$$\mathbf{K}_{T\mu}^\pm=(q,0,\pm k_{T\mu}), \quad \mu=A,B, \quad (5)$$

where  $q$  and  $k_{T\mu}$  are the  $x$  and  $z$  component of the wave vectors, which satisfy the following equation:

$$k_{T\mu}^2=(\omega/c)^2\epsilon_{T\mu}(\omega)-q^2, \quad \mu=A,B, \quad (6)$$

here  $q$  is given by

$$q=(\omega/c)\sin\theta, \quad (7)$$

where  $\theta$  is the incident angle, and  $c$  is the speed of light in vacuum. The function  $\epsilon_{T\mu}$  in Eq. (6) is the transverse dielectric function for the metal layer. In order to take account of the retardation effect on the system, we still adopt the model dielectric function in the form of the Drude local dielectric function for the metal layers in the MFSL,

$$\epsilon_{T\mu}(\omega)=1-\frac{\omega_{P\mu}^2}{\omega^2+i\omega/\tau_\mu}, \quad \mu=A,B, \quad (8)$$

where  $\tau_\mu$  is the electric relaxation time in the metallic layers, and  $\omega_{P\mu}$  is the plasma frequency for the two sorts of metal layers,

$$\omega_{P\mu}=(4\pi n_\mu e^2/m_e)^{1/2}, \quad \mu=A,B, \quad (9)$$

where  $n_\mu$  and  $m_e$  are the electron density and electron mass of the metal layers, respectively.

In the metallic layer, there are also two longitudinal waves with the wave vectors

$$\mathbf{K}_{L\mu}^\pm=(q,0,\pm k_{L\mu}), \quad \mu=A,B, \quad (10)$$

obeying

$$\epsilon_{L\mu}(\mathbf{K}_{L\mu}^\pm,\omega)=0, \quad (11)$$

where  $\epsilon_{L\mu}$  is a spatially dispersive longitudinal dielectric

function, which is given by<sup>6</sup>

$$\epsilon_{L\mu}(\omega)=1-\frac{\omega_{P\mu}^2}{\omega^2+i\omega/\tau_\mu-\beta_\mu^2 K_{L\mu}^2}, \quad (12)$$

where  $\beta^2=3v_F^2/5$  with  $v_F$  the Fermi velocity of the metal.

We assume that anywhere inside the metal layer of thickness  $d_\mu$  the field is given by a superposition of these four waves. Hence the field is determined by any four independent components at one point. As in Ref. 6, the corresponding four  $z$ -dependent components can be chosen as  $B_T^\pm$  and  $\phi_L^\pm$ , respectively; here  $\phi$  is the scalar potential in the Coulomb gauge. For the two interfaces of the metal layer in MFSL, they are related through

$$\begin{pmatrix} B_T^+ \\ B_T^- \\ \phi_L^+ \\ \phi_L^- \end{pmatrix}_{\text{left}} = \underline{T}_\mu \begin{pmatrix} B_T^+ \\ B_T^- \\ \phi_L^+ \\ \phi_L^- \end{pmatrix}_{\text{right}}, \quad \mu=A,BL,BS, \quad (13)$$

where

$$\underline{T}_\mu = \text{diag}(e^{-ik_{T\mu}d_\mu}, e^{ik_{T\mu}d_\mu}, e^{-ik_{L\mu}d_\mu}, e^{ik_{L\mu}d_\mu}). \quad (14)$$

For convenience, one can also substitute the related four independent electromagnetic field quantities  $E_x$ ,  $B_y$ ,  $E_z$ , and  $\phi$  for  $B_T^\pm$  and  $\phi_L^\pm$  at any point in the metal layer through

$$\begin{pmatrix} E_x \\ B_y \\ E_z \\ \phi \end{pmatrix}_z = \underline{G}_\mu \begin{pmatrix} B_T^+ \\ B_T^- \\ \phi_L^+ \\ \phi_L^- \end{pmatrix}_z, \quad \mu=A,BL,BS, \quad (15)$$

where

$$\underline{G}_\mu = \begin{pmatrix} Z_\mu & -Z_\mu & -iq & -iq \\ 1 & 1 & 0 & 0 \\ -W_\mu & -W_\mu & -ik_{L\mu} & ik_{L\mu} \\ 0 & 0 & 1 & 1 \end{pmatrix}, \quad (16)$$

with

$$Z_\mu = \frac{k_{T\mu}c}{\epsilon_{T\mu}\omega}, \quad W_\mu = \frac{qc}{\epsilon_{T\mu}\omega}. \quad (17)$$

The combination of Eqs. (13) and (15) leads to a  $4 \times 4$  transfer-matrix  $\underline{M}_\mu$  for the electromagnetic waves propagating through a metal layer of thickness  $d_\mu$  along the  $z$  direction in the MFSL,

$$\underline{M}_\mu = \underline{G}_\mu \underline{T}_\mu \underline{G}_\mu^{-1}, \quad (18)$$

which satisfies

$$\begin{pmatrix} E_x \\ B_y \\ E_z \\ \phi \end{pmatrix}_{\text{left}} = \underline{M}_\mu \begin{pmatrix} E_x \\ B_y \\ E_z \\ \phi \end{pmatrix}_{\text{right}}, \quad \mu=A,BL,BS. \quad (19)$$

By using the above equation to the positions of all inter-

faces and the two surfaces  $z_0$  and  $z_N$  for the system, we can obtain the relation for the electromagnetic waves through an  $n$ th generation MFSL as

$$\begin{pmatrix} E_x \\ B_y \\ E_z \\ \phi \end{pmatrix}_{z_0} = \underline{C}_n \begin{pmatrix} E_x \\ B_y \\ E_z \\ \phi \end{pmatrix}_{z_N}, \quad (20)$$

where  $\underline{C}_n$  is the  $n$ th-order transfer matrix, which is generated in agreement with the Fibonacci sequence,

$$\underline{C}_n = \underline{C}_{n-1} \underline{C}_{n-2}, \quad (21)$$

with the two initial generating seeds for the two elementary blocks of the MFSL,

$$\underline{C}_0 = \underline{M}_A \underline{M}_{BS}, \quad \underline{C}_1 = \underline{M}_A \underline{M}_{BL}. \quad (22)$$

If we let the  $n$ th finite MFSL act as a unit cell, and stack it repeatedly in the  $z$  direction infinitely, i.e., in the rational approximation,<sup>17</sup> we can obtain the electromagnetic normal modes of the system in the form of Bloch waves, which means

$$\begin{pmatrix} E_x \\ B_y \\ E_z \\ \phi \end{pmatrix}_{z_0} = e^{-ipD_n} \begin{pmatrix} E_x \\ B_y \\ E_z \\ \phi \end{pmatrix}_{z_N}, \quad (23)$$

where  $p$  is the Bloch wave vector. Comparing Eq. (20) with Eq. (23), we finally obtain the dispersion relation  $p = p(\omega)$  as follows:

$$\det(\underline{C}_n - e^{-ipD_n} \underline{I}) = 0, \quad (24)$$

where  $\underline{I}$  is a unit matrix. From Ref. 6 one can rewrite the dispersion relation in the following simple form:

$$4 \cos^2(pD_n) + 2\alpha_n \cos(pD_n) + \alpha'_n - 2 = 0, \quad (25)$$

where the two coefficients are

$$\alpha_n = -\text{Tr}(\underline{C}_n) \quad (26)$$

and

$$\alpha'_n = [\text{Tr}(\underline{C}_n)^2 - \text{Tr}(\underline{C}_n^2)]/2, \quad (27)$$

respectively. As the transfer matrices are all complex matrices due to the dielectric functions we used, the Bloch wave vector is now also a complex vector.

### III. NUMERICAL RESULTS AND DISCUSSIONS

In Sec. II we have presented formal equations for calculating the dispersion relation of electromagnetic normal modes of a metallic Fibonacci superlattice. But one need note that Eq. (25) is quadratic in  $\cos(pD_n)$ , i.e., there are two solutions for each frequency. In the real case of the numerical calculation, these can be sorted out according to the imaginary part of Bloch's wave vector  $p$ .

In order to compare the present results with our previous works, we still consider the layer  $A$  as metal Mg, and layer  $B$  as metal Al, and let the thicknesses of the metal

layers be  $d_A = 100 \text{ \AA}$ , and  $d_{BL} = 200 \text{ \AA}$ , respectively. For metal Mg, we take electron density  $n_A$  as  $8.63 \times 10^{22} \text{ cm}^{-3}$ , and for metal Al, we take electron density  $n_B$  as  $18.1 \times 10^{22} \text{ cm}^{-3}$ . As used in Refs. 6 and 15, we choose the electronic relaxation times as  $\tau_\mu = 100/\omega_{p\mu}$ . The stiffness constants for the two elementary metal layers are chosen to be  $\beta_A = 0.04c$  and  $\beta_B = 0.05c$ , respectively. For convenience, we set frequencies in units of  $\omega_{PB}$ , and  $q$  in units of plasma wave vector  $k_{PB}$ .

For the special case of  $q = 0.5k_{PB}$ , we plotted two pairs of calculated curves of the dispersion relation  $\omega$  versus  $p$  of metallic superlattice with a periodic unit cell of a fifth generation MFSL in Figs. 1 and 2. Figure 1 displays the solution with smaller imaginary part, while Fig. 2 is for the solution with bigger imaginary part. In the two figures, the real parts of  $p$  are shown in the left-hand side panel and its imaginary parts in the right-hand side panel. The real and imaginary parts of  $p$  are in units of  $\pi/D_n$  and  $F_n/D_n$ , respectively. One should note that we have used logarithmic scales for imaginary parts of the figures.

Comparing with our recent work for the  $s$ -polarized electromagnetic modes,<sup>16</sup> we found that Fig. 1 mainly gives information about the propagating transverse wave modes, which demonstrate the pattern of the reflectivity (see Fig. 1) if one maps the forbidden frequency bands of the real part  $p$  (see the left-hand side panel) to the reflection maxima,<sup>16</sup> and Fig. 2 corresponds to the longitudinal modes with much smaller frequency gaps and bands compared with Fig. 1. We denote these two modes as PTM (propagating transverse wave mode) and PLM (propagating longitudinal wave mode), respectively.

From our numerical calculations, we found the first very interesting result that similar to the pattern of reflectance spectra, both the real and imaginary parts of the PTM pattern in the region of  $p$ -polarized soft x rays

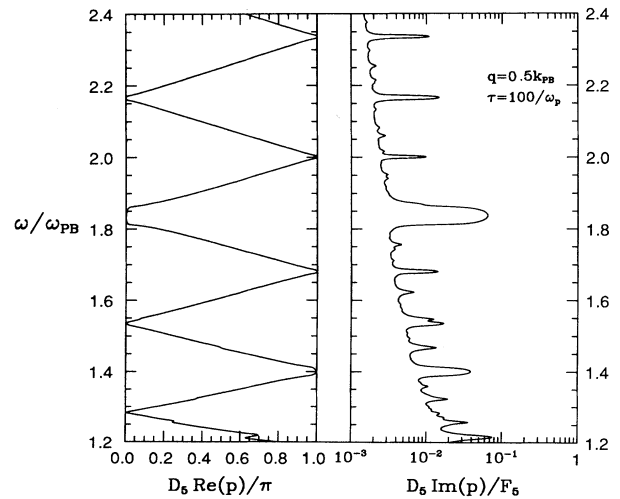


FIG. 1. Dispersion relation  $\omega$  vs complex vector  $p$  of small imaginary part modes for a superlattice with a periodic unit cell of a fifth generation MFSL. The relevant parameters are  $d_A = 100 \text{ \AA}$ ,  $d_{BL} = 200 \text{ \AA}$ ,  $\tau = 100/\omega_p$ ,  $q = 0.5k_{PB}$ , and  $\omega_{PB}$  is the plasma frequency for metal Al.

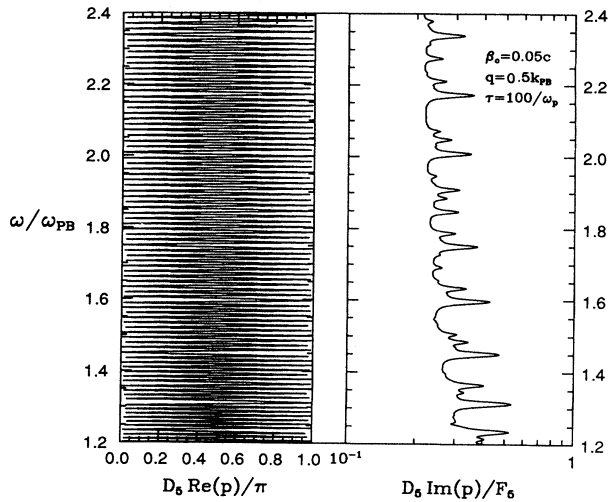


FIG. 2. Dispersion relation  $\omega$  vs complex vector  $p$  of large imaginary part modes according to the same parameters as in Fig. 1. Note the different logarithm scale for the imaginary part of the figure.

and ultraviolet has a rich structure of self-similarity. When  $n$  approaches infinity, all the normal modes become clearly critical (neither extended nor localized), and the allowed frequency bands for the real part of  $p$  form a Cantor-like set. One can clearly see the situation of self-similarity from Fig. 3, where we show the two-generation curves of the dispersion relation  $\omega$  against the imaginary part  $p$  for PTM. The two-generation numbers  $n$  for the

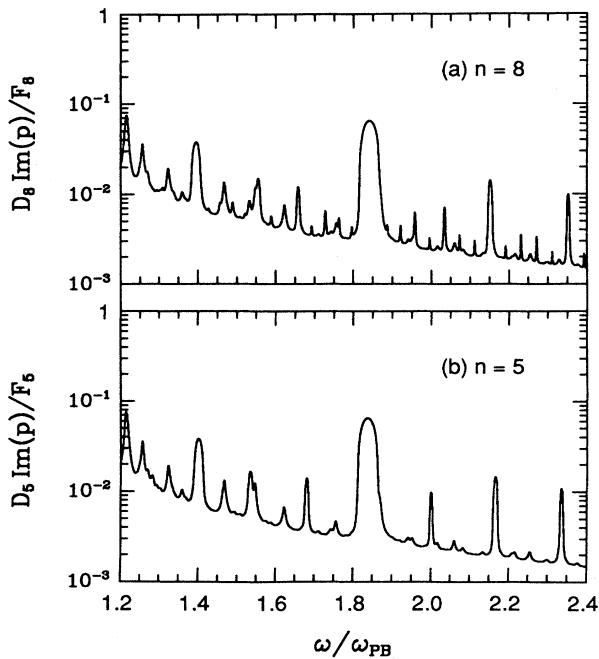


FIG. 3. Dispersion relation of small imaginary part  $\text{Im}(p_n)$  vs  $\omega$  for the superlattice with two-generation MFSL unit cells (a)  $n=8$ , (b)  $n=5$ . The relevant parameters are the same as Fig. 1.

unit cell of MFSL are 8 and 5, respectively. The frequency scaling change, which is the same as that in the spectra pattern of the reflectivity,<sup>14,15</sup> shows that the PTM is strongly dependent on the Fibonacci geometrical structure. But when  $q/k_{PB}$  decreases (see Fig. 4), which means enhancing the retardation effect, the self-similarity of the dispersion spectra will be restrained strongly in the low-frequency range with increasing generation number, which coincides with the behavior of the reflectivity spectra.<sup>15</sup>

Next we found that in the region of  $\omega > \omega_{PB}$  the imaginary part of vector  $p$  for PLM is approximately of the following form:

$$\text{Im}(p_n) = \mathcal{P}(\omega)(F_n/D_n), \quad (28)$$

where  $\mathcal{P}(\omega)$  is an  $n$ -independent function, which suggests that one can call  $D_n/F_n$  a quasiperiodic modulation length. One can draw the conclusion from Fig. 5. Another property we revealed is that both the real and imaginary parts of  $p$  of PLM are approximately  $q$  independent for the frequency region above  $\omega_{PB}$  (see the dashed curves in Fig. 4), which confirms the longitudinal resonance for PLM in the metallic layers.

Finally, we found that in the region from  $\omega_{PA}$  to  $\omega_{PB}$  the electromagnetic normal modes become much more complicated compared with that in the region  $\omega > \omega_{PB}$ . For the frequency region near the plasma frequency of metal B, there will be overlaps between PTM and PLM, which reveal the behavior of strong coupling between

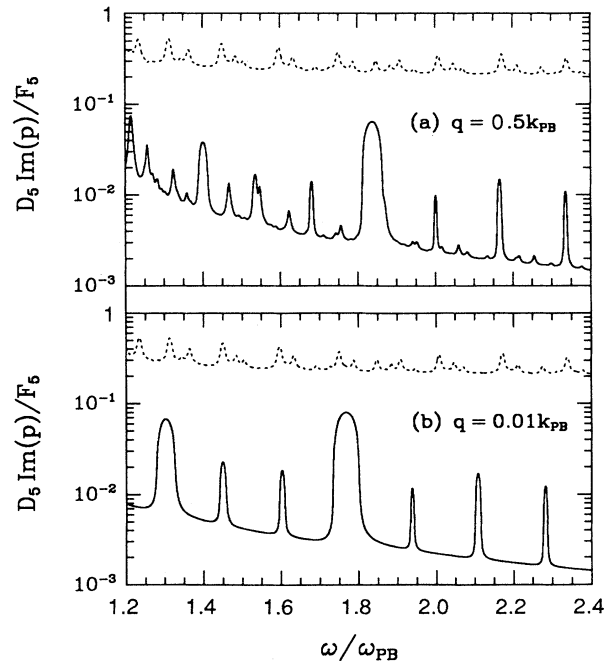


FIG. 4. Dispersion relation of the imaginary part  $\text{Im}(p_n)$  vs  $\omega$  for the superlattice with two different  $x$ -component wave vectors (a)  $q/k_{PB}=0.5$ , (b)  $q/k_{PB}=0.01$ . The dashed line is for PLM and the solid line for PTM. The other parameters are the same as Fig. 1.

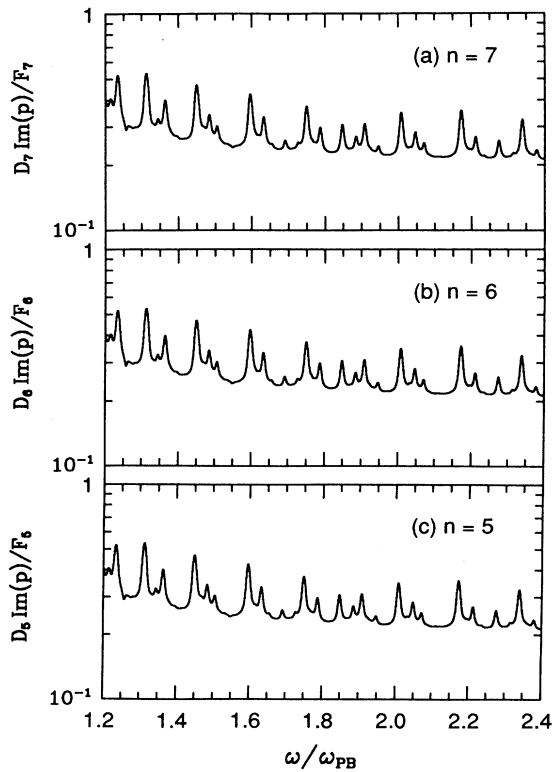


FIG. 5. The same as in Fig. 3 but for the large imaginary part of dispersion relation with three-generation MFSL unit cells (a)  $n=7$ , (b)  $n=6$ , (c)  $n=5$ .

transverse waves and longitudinal waves. For the case of low-generation MFSL, for example,  $n=3$ , and when  $\omega_{PA} < \omega < \omega_{PB}$ , the interface plasma modes, as identified in Ref. 6 for the situation of periodic conductor superlattice, will appear in the dispersion relation. The imaginary parts of  $p$  versus  $\omega$  for PLM will exist as a series of minima. At the corresponding positions of the minima, there are sharp peaks for the real parts of  $p$  versus  $\omega$ ; those modes are made up of guided plasmons in the metal  $A$  layers. Due to the quasiperiodic design of our model, the analytical expression for the resonant position, not like the usual standard periodic superlattice,<sup>6</sup> cannot be simply given out. The very interesting property we found is that when  $n$  increases, both the real and imaginary part of PLM will be modulated by a series of sharp fluctuation. Figure 6 shows the modes with sharp fluctuation in an enlarged scale. The pair of the cloudlike points in Fig. 6 corresponds to PTM. We believe that this peculiar optical phenomenon is also caused by the quasiperiodic structure of a Fibonacci superlattice.

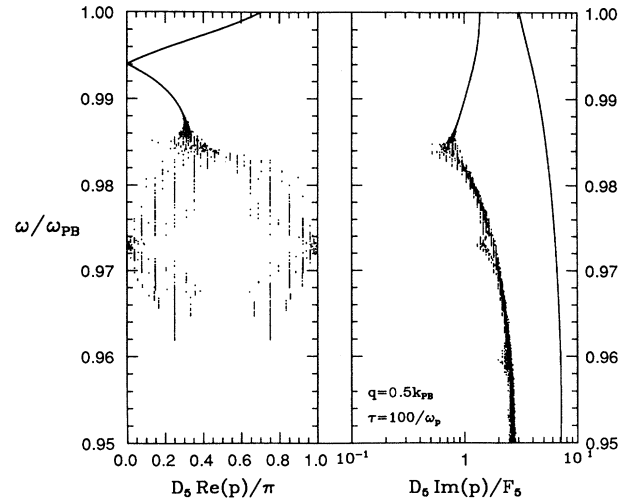


FIG. 6. Dispersion relation  $\omega$  vs complex vector  $p$  for a superlattice with a periodic unit cell of a fifth generation MFSL. The relevant parameters are the same as Fig. 1 but with the different frequency range.

#### IV. CONCLUSION

In conclusion, the optical properties of a metallic Fibonacci superlattice have been studied for the region of  $p$ -polarized soft x rays and the extreme ultraviolet by using the  $4 \times 4$  transfer-matrix method. The retardation effect to the system and the coupling between the transverse waves and longitudinal waves is considered and we have presented in detailed formalism the dispersion relation. It is shown that within the rational approximation, the electromagnetic normal modes become critical, i.e., the dispersion spectra are self-similar as the generation number and  $q$  increase greatly. But for small  $q$ , the self-similarity of the dispersion spectra will be restrained due to the retardation effect on the system and the strong coupling between the transverse and longitudinal waves. The interface plasmon modes we found are much more complicated compared with that in the usual periodic system.

#### ACKNOWLEDGMENTS

We gratefully acknowledge many helpful discussions with Dr. Hong Chen. One of the authors (W.F.) would like to thank Professor Abdus Salam, the International Atomic Energy Agency, and UNESCO for hospitality at the International Centre for Theoretical Physics, Trieste, Italy. Part of this work was supported by the Chinese National Advanced Technology Foundation through Grant No. 040-144-05-085.

<sup>1</sup>Chien-Hua Tsai *et al.*, *Proceedings of the Workshop on the Physics of Superlattice and Quantum Well* (World Scientific, Singapore, 1989).

<sup>2</sup>P. J. Steinhardt and S. Ostlund, *The Physics of Quasicrystals* (World Scientific, Singapore, 1987).

<sup>3</sup>R. E. Camley and D. L. Mills, *Phys. Rev. B* **29**, 1695 (1984).

<sup>4</sup>B. L. Johnson, J. T. Weiler, and R. E. Camley, *Phys. Rev. B* **32**, 6544 (1985).

<sup>5</sup>H. Shi and J. H. Tsai, *Acta Phys. Sin.* **37**, 683 (1988).

<sup>6</sup>W. Luis Mochán and Marcelo del Castillo-Mussot, *Phys. Rev. B* **35**, 1088 (1987); **37**, 6763 (1988); Marcelo del Castillo-Mussot and W. Luis Mochán, *ibid.* **36**, 1779 (1987).

- <sup>7</sup>P. Hawrylak, G. Eliasson, and J. J. Quinn, *Phys. Rev. B* **36**, 6501 (1987).
- <sup>8</sup>M. Kohmoto, B. Sutherland, and K. Iguchi, *Phys. Rev. Lett.* **58**, 2436 (1987).
- <sup>9</sup>R. Merlin, K. Bajema, R. Clarke, F. Y. Juang, and P. K. Bhattacharya, *Phys. Rev. Lett.* **55**, 1768 (1965).
- <sup>10</sup>J. Feng, Y. Zhu, and N. Ming, *Phys. Rev. B* **41**, 5578 (1990).
- <sup>11</sup>L. Tang, *Phys. Rev. Lett.* **64**, 2390 (1990).
- <sup>12</sup>J. Q. You and Q. B. Yang, *J. Phys. Condens. Matter* **2**, 2093 (1990).
- <sup>13</sup>F. Frostman, *Z. Phys.* **32**, 385 (1975); C. Schwartz and W. L. Schaich, *Phys. Rev. B* **26**, 7008 (1982); P. Ahqvist and P. Apell, *Phys. Scr.* **25**, 587 (1982).
- <sup>14</sup>Wei-guo Feng, Wen-zhong He, Deng-ping Xue, Yi-bing Xu, and Xiang Wu, *J. Phys. Condens. Matter* **1**, 8241 (1989).
- <sup>15</sup>Wei-guo Feng, He-sheng Yao, and Xiang Wu, *J. Phys. Condens. Matter* **2**, 6547 (1990).
- <sup>16</sup>Wei-guo Feng, Nian-hua, Liu and Xiang Wu, *Commun. Theor. Phys.* **14**, 1 (1990).
- <sup>17</sup>M. Kohmoto, L. P. Kadanoff, and C. Tang, *Phys. Rev. Lett.* **50**, 1870 (1983).